

Improved Fe/Mg–Al hydrotalcite catalyst for Baeyer–Villiger oxidation of ketones with molecular oxygen and benzaldehyde

Tomonori Kawabata^a, Naoko Fujisaki^a, Tetsuya Shishido^b, Kiyoshi Nomura^c,
Tsuneji Sano^a, Katsuomi Takehira^{a,*}

^a Department of Chemistry and Chemical Engineering, Graduate School of Engineering, Hiroshima University,
Kagamiyama 1-4-1, Higashi-Hiroshima 739-8527, Japan

^b Department of Molecular Engineering, Graduate School of Engineering, Kyoto University, Katsura 1, Saikyo-ku, Kyoto 615-8510, Japan

^c School of Engineering, University of Tokyo, Hongo 7-3-1, Bunkyo-ku, Tokyo 113-8656, Japan

Received 18 February 2006; received in revised form 30 March 2006; accepted 31 March 2006

Available online 5 May 2006

Abstract

Metal (Me: Fe, Co, Ni or Cu) containing Mg–Al hydrotalcite-type anionic clay catalysts have been prepared by adopting the “memory effect” of hydrotalcite and tested for Baeyer–Villiger oxidation of ketones. Mg–Al hydrotalcite was calcined to the mixed oxide and dipped in an aqueous solution of metal (Me) salt; metal species was incorporated by “memory effect” to form Me/Mg–Al hydrotalcite as the active phase on the surface of the Mg–Al mixed oxide. The activity and the structure of these catalysts have been compared with those of metal supported catalysts prepared by coprecipitation and impregnation. Among the metals tested, iron was the most effective and use of $\text{Fe}(\text{NH}_4)_2(\text{SO}_4)_2 \cdot 6\text{H}_2\text{O}$ as the metal salt resulted in the highest activity. The activity of the catalyst was higher than those prepared by coprecipitation from the nitrates of Mg, Fe and Al. Judging from Mössbauer and Fe K-edge XAFS spectra, Fe species possess the Fe^{3+} valence state, are mainly octahedrally coordinated and form Fe–O–Fe cluster-type structure on the Mg–Al mixed oxides. This clearly indicates that the Fe^{3+} –O– Fe^{3+} cluster-type compounds are more active for the Baeyer–Villiger oxidation than well dispersed Fe^{3+} species formed on the hydrotalcite prepared by coprecipitation. Six-membered cyclic ketones, such as cyclohexanone, 2-norbornone and 2-adamantanone, were effectively oxidized to the corresponding lactones by using O_2 /benzaldehyde as an oxidizing agent.

© 2006 Elsevier B.V. All rights reserved.

Keywords: Mg–Al hydrotalcite; Cluster-iron oxide; Memory effect; Baeyer–Villiger oxidation; Oxygen; Benzaldehyde

1. Introduction

Baeyer–Villiger (B–V) oxidation of ketones is widely used for the synthesis of various lactones or esters. B–V reactions have been commonly carried out using peracid oxidants, such as persulfuric acid, perbenzoic acid, *m*-chloroperbenzoic acid (*m*-CPBA) and hydrogen peroxide [1–5]. Homogeneous catalysts have been tested for various types B–V reactions [6] and such works are recently rather focusing on regio- or enantioselective oxidations [7–9]. Heterogeneous catalysts have the following advantages over the homogeneous catalysis: (1) simplicity in synthetic operations, (2) prevention of the production of salt wastes during neutralization of the catalysts or reagents and (3)

reusability of the solid catalyst [10–12]. Organic ion exchange resins [13] or polymer-anchored Pt complexes [14] or Bi(III) triflate [15] have been used as catalysts with aqueous H_2O_2 solution. Corma et al. [16–18] reported that Sn/zeolite-beta was very active and selective for the B–V oxidation of cycloketones or aromatic aldehydes with H_2O_2 , leading to the synthesis of fragrance compounds. Natural clay minerals are environmentally benign and were frequently used as the catalyst support. Both palygorskite, $(\text{Mg},\text{Al})_5\text{Si}_8\text{O}_{20}(\text{OH})_2(\text{H}_2\text{O})_4 \cdot 4\text{H}_2\text{O}$, and hydrotalcite, $\text{Mg}_6\text{Al}_2(\text{OH})_{16}\text{CO}_3 \cdot 4\text{H}_2\text{O}$, possess Mg^{2+} and Al^{3+} sites that are octahedrally coordinated and can be easily exchanged. Sn-exchanged palygorskite [19] and Sn-exchanged Mg–Al hydrotalcite [20] are active and selective for the B–V oxidation of cyclic ketones with H_2O_2 .

A combination of molecular oxygen and aldehydes under heterogeneous catalysis has also been extensively studied [21–26] since Kaneda et al. [27] reported the oxidative cleavage of

* Corresponding author. Tel.: +81 82 424 7744; fax: +81 82 424 7744.
E-mail address: takehira@hiroshima-u.ac.jp (K. Takehira).

alkenes into carbonyl compounds over RuO₂–CH₃CHO–O₂ system. We have recently reported the B–V reaction of ketones and the alcohol oxidation using the heterogeneous iron-containing MCM-41 [28] and Ni-containing Mg–Al hydrotalcite [29] catalysts, respectively. Both Ni/Mg–Al and Fe–MCM-41 possessed isolated Ni and Fe sites which are coordinated octahedrally and tetrahedrally, respectively, with oxygen atoms. The latter catalyst worked as Lewis acid for the B–V reactions with O₂/PhCHO system at low reaction temperatures, and the catalyst was reusable without any appreciable loss in its activity and selectivity. The use of iron metal as catalytically active species is significantly attractive because the iron-containing compounds generally show low toxicity [30] and are easily available. Mg–Al hydrotalcite can capture iron species in the structure since the Mg–Al system is the most common hydrotalcite compounds, in which various metal cations can substitute both of Mg(II) and Al(III) sites depending on the valence state and the ionic radii [31]. Kaneda et al. [32] reported that Mg–Al–Fe hydrotalcite prepared by coprecipitation was active for the B–V oxidation of cyclic ketones whereas a replacement of Fe by Cu in the hydrotalcite produced an active catalyst for the B–V oxidation of bicyclic ketones. In these reactions, basic sites on the Mg–Al hydrotalcite was supposed to be important for oxygen transfer from perbenzoic acid to ketone [33].

The hydrotalcites also exhibit a striking property termed “memory effect” in which the products of their thermal decompositions experience a spontaneous structural reconstitution when put in aqueous medium. This phenomenon was observed in Mg–Al and Zn–Al hydrotalcites [34], and it is, particularly,

well-known in Mg–Al based hydrotalcites [35–37]. By adopting the “memory effect,” we succeeded in surface enrichment of the active species on the catalyst particles, i.e. in the preparation of “egg shell” type loaded Ni/Mg–Al catalyst [38–40]. Mg–Fe hydrotalcites are currently attracting interest as catalyst precursors [41–43] and has been used for the Fisher-Tropsch reaction after decomposition followed by reduction [42]. It was confirmed that “memory effect,” i.e. reconstitution takes place after the decomposition of Mg–Fe hydrotalcites [44,45]. In the present paper, we report the preparation of Fe³⁺ containing Mg–Al hydrotalcites by the reconstitution and their catalytic behavior in the B–V oxidation of ketones with molecular oxygen and benzaldehydes.

2. Experimental

2.1. Catalyst preparation

Procedure of catalyst preparation and its property was shown in Table 1. Mg–Al hydrotalcites, [Mg(II)_{1-x}Al(III)_x(OH)₂]^{x+}(CO₃²⁻)_{x/2}·nH₂O, were prepared by coprecipitation reported by Miyata and Okada [46] with minor modification. An aqueous solution of the nitrates of Mg(II) and Al(III) was added slowly with vigorous stirring into an aqueous solution of sodium carbonate at 333 K. By adjusting the pH of this solution to 10 with an aqueous solution of sodium hydroxide, heavy slurry precipitated. The crystal growth took place by aging the solution at 333 K for 24 h. After the solution was cooled to room temperature, the precipitate was washed

Table 1
Preparation and properties of metal containing Mg–Al hydrotalcite

Lot No.	Catalyst	Preparation method	Concentration of metal (M) ^a	pH of metal solution	Metal loading (wt%) ^b	Molar ratio ^b			BET surface area (m ² g _{cat} ⁻¹)	Color
						Mg	Al	Me		
1	Mg ₃ Al-HT(as syn.)	–	–	–	–	3.0	1.0	–	99.1	White
2	Mg ₃ Al(cal.)	–	–	–	–	3.0	1.0	–	150.0	White
3	Fe/Mg ₃ Al-M ^c	Memory	0.03	1.5	9.6	2.2	1.0	0.5	58.0	Brown
4	Co/Mg ₃ Al-M ^c	Memory	0.03	3.0	2.4	2.9	1.0	0.1	8.7	Dark grey
5	Ni/Mg ₃ Al-M ^c	Memory	0.03	3.0	4.1	2.9	1.0	0.2	6.0	Light green
6	Cu/Mg ₃ Al-M ^c	Memory	0.03	3.0	2.2	3.0	1.0	0.1	39.8	Light blue
7	Fe/Mg ₃ Al-M ^d	Memory	0.03	1.5	11.1	2.2	1.0	0.5	49.6	Brown
8	Fe/Mg ₃ Al-M ^e	Memory	0.3	3.0	10.6	2.4	1.0	0.6	11.9	Dark ocher
9	Fe/Mg ₃ Al-M ^e	Memory	0.1	3.0	10.6	2.4	1.0	0.6	12.7	Dark ocher
10	Fe/Mg ₃ Al-M ^e	Memory	0.03	3.0	6.1	2.7	1.0	0.4	18.5	Dark ocher
11	Fe/Mg ₃ Al-M ^e	Memory	0.01	3.0	3.5	2.9	1.0	0.2	14.5	Ocher
12	Fe/Mg ₃ Al-M ^e	Memory	0.005	3.0	1.5	3.0	1.0	0.1	5.8	Light ocher
13	Fe/Mg ₁ Al-M ^e	Memory	0.03	3.0	10.3	0.7	1.0	0.3	6.8	Dark ocher
14	Fe/Mg ₆ Al-M ^e	Memory	0.03	3.0	8.0	4.7	1.0	0.9	78.8	Dark ocher
15	Fe/Mg ₃ Al-CP ^f	Coprecipitation	–	10.0	7.9	2.9	1.0	0.4	64.5	Light ocher
16	Fe/Mg ₂ Al-CP ^f	Coprecipitation	–	10.0	6.9	1.8	1.0	0.4	95.5	Light ocher
17	Fe/Mg ₃ Al-HT ^g	Impregnation	0.03	3.0	6.4	1.2	1.0	0.2	12.5	Ocher
18	Fe/γ-Al ₂ O ₃	Impregnation	0.03	–	8.5	–	1.0	0.1	132.2	Light ocher
19	Fe/MgO	Impregnation	0.03	–	8.7	1.0	–	0.2	30.8	Light ocher

^a Molar concentration of aqueous solution of metal salts used for the catalyst preparation.

^b Obtained by ICP analyses.

^c Mg₃Al(cal.) was dipped in aqueous solution of the nitrate of each metal for 15 min.

^d Mg₃Al(cal.) was dipped in aqueous solution of Fe(NO₃)₃·9H₂O for 60 min.

^e Mg₃Al(cal.) was dipped in aqueous solution of Fe(NH₄)₂(SO₄)₂·6H₂O for 60 min.

^f Prepared by coprecipitation of Mg(NO₃)₂·6H₂O, Al(NO₃)₃·9H₂O and Fe(NO₃)₃·9H₂O at pH 10.0.

^g Mg₃Al-HT as synthesized was dipped in aqueous solution of Fe(NH₄)₂(SO₄)₂·6H₂O for 60 min.

with deionized water, dried at 373 K for 24 h and calcined at 1123 K (0.83 K min^{-1}) for 5 h in air to form powder of Mg–Al mixed oxides, which were used as the carrier for the preparation of Fe-supported catalysts. As controls, the calcinations at 923 and 1223 K were also tested for the preparation of Mg–Al mixed oxides powder.

Supported Fe catalysts were prepared by adopting the “memory effect” as follows: 1.0 g of Mg–Al mixed oxide powder was dipped in 100 ml aqueous solution of $\text{Fe}(\text{NH}_4)_2(\text{SO}_4)_2 \cdot 6\text{H}_2\text{O}$ and the mixed solution was slowly stirred for 15–60 min at room temperature. At the beginning, pH of the solution was fixed at 3.0 by adding 1 M HNO_3 aqueous solution. The concentration of aqueous solution of $\text{Fe}(\text{NH}_4)_2(\text{SO}_4)_2 \cdot 6\text{H}_2\text{O}$ was varied between 0.005 and 0.3 M depending on the loading amount of Fe. After the dipping, the solid materials were separated by filtration, washed with 1 l of deionized water, dried at 353 K for 24 h and used as the catalyst. The Fe-supported catalysts were denoted as Fe/Mg₃Al–M, where Mg–Al hydrotalcite was reconstituted by the “memory effect” and covered the surface of Mg–Al mixed oxides during the dipping (vide infra). As controls, Co, Ni and Cu/Mg₃Al–M were prepared in a similar way by using the nitrates of Co(II), Ni(II) and Cu(II) at pH 3.0 adjusted by adding 1 M HNO_3 , whereas Fe/Mg₃Al–M was prepared by using Fe(III) nitrate at pH 1.5 since pH of the solution was originally 1.5 and could not be adjusted at 3.0 by adding 1 M HNO_3 .

Fe-containing Mg–Al hydrotalcite as a control was also prepared by coprecipitation from the nitrates of Fe(III), Mg(II) and Al(III) at pH 10.0 [40] and designated as Fe/Mg₃Al–CP. Fe/ γ -Al₂O₃ and Fe/MgO catalysts were prepared as a control by impregnation of ALO-8 and MgO, respectively, with Fe(III) nitrate aqueous solution. The powder after impregnation was dried at 353 K for 5 h, followed by vacuum drying at 313 K for 4 h, and used as the control catalyst. Fe₂O₃ and Fe₃O₄ were used as purchased.

2.2. Characterization of the catalyst

The structures of the catalysts were studied by XRD, Fe K-edge XAFS, Mössbauer, ICP, UV–vis and a N₂-adsorption method.

Powder X-ray diffraction (XRD) measurements were performed with a Rigaku Powered Diffraction Unit, RINT2250VHF with Cu K α radiation (40 kV, 300 mA). The diffraction patterns were identified by comparing with those included in the Joint Committee of Powder Diffraction Standards (JCPDS) data base.

The Fe K-edge X-ray absorption spectra were measured at the BL-01B1 at SPring-8, Hyogo, Japan. The data were recorded in transmission mode at room temperature using Si(1 1 1) double crystal monochromator. Energy was calibrated with Cu K-edge absorption (8981.0 eV), and the energy step of measurement in the XANES region was 0.3 eV. The data analysis was performed using the REX2000 Ver. 2.3 (Rigaku). For the extended X-ray absorption fine structure (EXAFS) analysis, the oscillation was extracted from the EXAFS data by a spline smoothing method [47]. The oscillation was normalized by edge height

around 50 eV higher than the absorption edge. The sample was mixed with boron nitride as a binder and pressed into a disk (10 mm in diameter).

⁵⁷Fe transmission Mössbauer spectra of pelletized powder samples were recorded at room temperature, using a constant acceleration mode (Topologic System Co.) of a radiation source with about 40 MBq ⁵⁷Co(Cr) and a YAP scintillation counter. Doppler velocity was calibrated with reference to α -Fe.

The ICP measurements were carried out using a Perkin-Elmer OPTIMA 3000. The content of metal component was determined after the sample was completely dissolved using diluted hydrochloric acid and a small amount of hydrofluoric acid.

The diffuse reflectance UV–vis spectra were recorded on a Perkin-Elmer UV/VIS/NIR (Lambda 900) spectrophotometer. The powdery sample was loaded into a quartz cell, and the spectra were collected at 200–700 nm referenced to BaSO₄.

N₂-adsorption (77 K) studies carried out with a Bell Japan BELSORP 18SP equipment (volumetric) were used to examine BET surface areas.

2.3. Catalytic testing

The Baeyer–Villiger oxidation of ketones was carried out using a batch-type reactor. In a typical reaction, 50 mg of catalyst was added to a glass flask precharged with cyclohexanone (1 mmol), benzaldehyde (3 mmol) and acetonitrile (10 ml). Oxygen (10 ml min^{-1}) was bubbled into the stirred solution. The heterogeneous reaction mixture was stirred at 45 °C for 15 h, and the catalyst was removed by filtration. The products in the filtrate were analyzed by GC (BPX-5, 30 M \times 0.25 mm).

3. Results and discussion

3.1. Properties of the catalysts

The physicochemical properties of MgAl-supported metal catalysts prepared by adopting the “memory effect” are shown in Table 1 together with those of Mg₃Al-HT, Mg₃Al mixed oxide and control catalysts. BET surface area of Mg₃Al-HT was as large as around $100 \text{ m}^2 \text{ g}^{-1}$ and increased to $150 \text{ m}^2 \text{ g}^{-1}$ after the calcination. After dipping the calcined Mg₃Al mixed oxide sample in metal solution, the surface area decreased significantly. Among Mg₃Al-supported metal catalysts, Fe/Mg₃Al–M showed relatively large surface area, followed by Cu/Mg₃Al–M, whereas both Co/Mg₃Al–M and Ni/Mg₃Al–M showed a drastic decrease in the surface area (Lot Nos. 3–6). Mg and Al metals were quantitatively incorporated in both Mg₃Al-HT as synthesized and Mg₃Al mixed oxide after calcination. When Co and Ni were supported on Mg₃Al mixed oxide (Lot Nos. 4 and 5), Mg content slightly decreased and small amount of Co and Ni were incorporated, while the Al content showed no detectable change, indicating that metal species replaced Mg sites. Whereas Cu/Mg₃Al–M apparently showed no decrease in the Mg content (Lot No. 6), it is likely that small amount of Cu replaced the Mg sites since Cu²⁺–Al³⁺ hydrotalcite-like layered structure is available (vide infra).

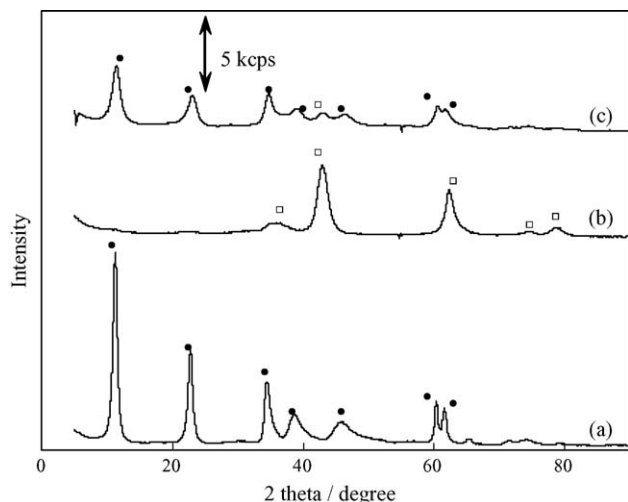


Fig. 1. XRD patterns of Fe(6.1 wt%)/Mg₃Al-M catalyst during preparation. (a) Mg₃Al HT after coprecipitation, (b) Mg₃Al mixed oxide after calcination at 1123 K for 5 h (0.83 K min⁻¹) and (c) Fe(6.1 wt%)/Mg₃Al-M catalyst after dipping, followed by drying. (●) Hydrotalcite and (□) Mg(Al)O periclase.

XRD patterns of Fe(6.1 wt%)/Mg₃Al-M catalyst (Lot No. 10) during the preparation by the “memory effect” are shown in Fig. 1. Mg₃Al-HT showed reflection lines typical of hydrotalcites (Fig. 1a) and changed to Mg(Al)O periclase after the calcination at 1123 K (Fig. 1b). After dipping the calcined sample in an aqueous solution of Fe(NH₄)₂(SO₄)₂·6H₂O, reflection lines of hydrotalcites appeared (Fig. 1c), indicating the reconstitution of hydrotalcites by the “memory effect.” The lines of hydrotalcites were not so intensive compared to the original Mg₃Al-HT, while the lines of Mg(Al)O were significantly broadened, suggesting that only a part of Mg(Al)O powder particle was reconstituted into hydrotalcites.

3.2. Metal loading

Whenever Fe, Co, Ni and Cu were used, the reconstitutions of hydrotalcite were observed by XRD after the dipping irrespective of the metal species. Among the four metals, Fe was most intensively loaded on the catalyst. However, pH was not kept at 3.0 in the Fe(III) nitrate solution (*vide infra*), resulting in a significant dissolution of Mg (Table 1, Lot No. 3). Even increase in the dipping time from 15 to 60 min showed only a small increase in the Fe loading (Lot No. 7). In the preparations of these metal-supported catalysts, the powder of Mg-Al mixed oxide was dipped into the aqueous solution of metal nitrate. Before the dipping, pH of the solution was adjusted to 3.0 by adding 1 M HNO₃ aqueous solution, which was the most profitable pH value for accelerating the reconstitution of hydrotalcites proceeding by the dissolution–recrystallization mechanism [39,40]. The pH values of aqueous solutions of the nitrates of Co(II), Ni(II) and Cu(II) were above 3.0 and adjusted to 3.0 by adding 1 M HNO₃, whereas aqueous solution of Fe(III) nitrate showed pH 1.5 and therefore alkaline, such as NaOH, was required for adjusting the pH to 3.0. However, alkaline addition possibly caused separate precipitation of Fe(III) hydroxide. As a result, an alternative compound, Fe(NH₄)₂(SO₄)₂·6H₂O, was used as

Fe source since the pH value of its aqueous solution was around 4.5 and was adjusted to 3.0 by adding 1 M HNO₃ (Lot Nos. 8–14). BET surface area of the Fe/Mg₃Al-M catalysts increased with increasing Fe concentration, reached the maximum value at 0.03 M and then decreased with the further increase. On the other hand, coprecipitated catalysts showed higher BET surface area than those prepared by the “memory effect” (Lot Nos. 15 and 16).

When the mixed oxides with the compositions of Mg₆Al, Mg₃Al and Mg₁Al as the catalyst supports were dipped in 0.03 M of Fe(NH₄)₂(SO₄)₂·6H₂O aqueous solution (Lot Nos. 13, 10 and 14), Fe loadings were rather low for the Mg₃Al compared with the others. In the XRD results (data not shown), the most intensive reconstitution was observed for the Mg₃Al composition, whereas the Mg₆Al and Mg₁Al showed rather weak intensities of hydrotalcite reflections; the reflections of MgAl₂O₄ spinel and Mg(Al)O periclase, respectively, were observed after the dipping. This may be due to the fact that the hydrotalcites layered structure is well stabilized around the Mg/Al ratio of 3/1 [48].

When the Fe loading was changed by changing the concentration of Fe(NH₄)₂(SO₄)₂·6H₂O solution, reflection intensities of hydrotalcites varied significantly after the dipping (Fig. 2). Low Fe concentration afforded rather intensive reflections of hydrotalcites. Intensities of hydrotalcites reflections decreased, reached a minimum value around 0.05 M (Fig. 2e), and then increased again with increasing Fe concentration in the solution. Moreover, reflection lines of Mg(OH)₂ appeared at high Fe concentration above 0.05 M. On the other hand, Fe loading

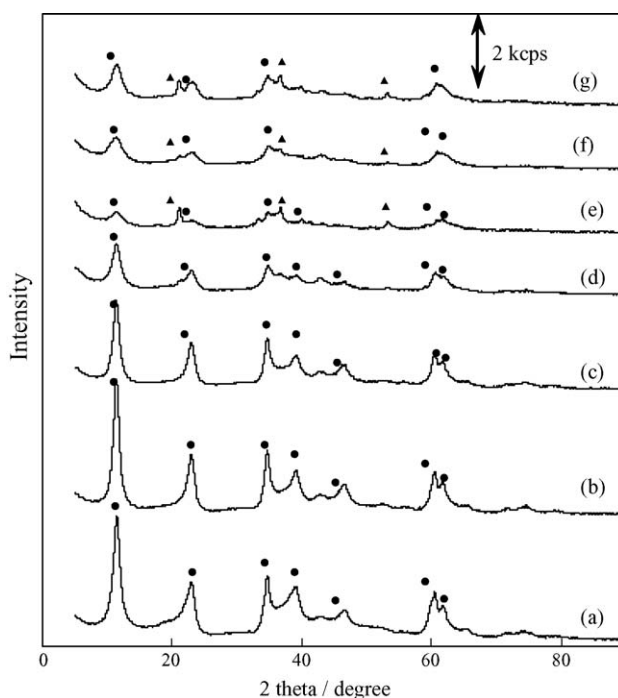


Fig. 2. XRD patterns of Fe/Mg₃Al-M catalysts prepared in varying Fe concentrations. (a) 0.001 M, (b) 0.005 M (1.5 wt%), (c) 0.01 M (3.5 wt%), (d) 0.03 M (6.1 wt%), (e) 0.05 M, (f) 0.1 M (10.6 wt%) and (g) 0.3 M (10.6 wt%). Number in the parenthesis is the Fe loading on the catalysts. (●) Hydrotalcite and (▲) Mg(OH)₂.

monotonously increased with increasing Fe concentration in the solution up to 0.1 M and the further increase up to 0.3 M resulted in saturation in Fe loading (Fig. 2f and g). These results indicate that the reconstitution is not essential for increasing the Fe loading.

3.3. Activity of the catalyst

Activities of metal-supported catalysts for the B–V oxidation of cyclohexanone are shown in Table 2. A blank test in the absence of catalyst showed low yield of ϵ -caprolactone (Run No. 20), and use of Mg₃Al-HT resulted in an increased yield (Run No. 19), showing that the B–V oxidation is catalyzed by Mg₃Al-HT itself probably as a base as reported [23,24]. It was reported that Mg–Al–Fe hydrotalcite prepared by coprecipitation was active for the B–V oxidation of cyclic ketones, whereas a replacement of Fe by Cu in the hydrotalcite produced an active catalyst for the B–V oxidation of bicyclic ketones [32]. Among Fe, Co, Ni and Cu/Mg₃Al-M catalysts (Run Nos. 1–4), Cu/Mg₃Al-M showed the highest activity, followed by Co, Ni and Fe/Mg₃Al-M. However, Cu/Mg₃Al-M led to significant leaching of Cu during the reaction, while no

leaching was observed for the other metals, Fe, Co and Ni. These catalysts were prepared by using the nitrates of respective metals, where pH of aqueous solution of Fe(III) nitrate could not be kept at 3.0, resulting in a low activity (Run No. 1) compared with those obtained for Fe/Mg₃Al-CP (Run No. 12); the latter catalyst was reported to be active by Kaneda et al. [32]. Use of Fe(NH₄)₂(SO₄)₂·6H₂O instead of Fe(III) nitrate resulted in an enormous increase in the activity and the highest activity was obtained for Fe(6.1 wt%)/Mg₃Al-M (Run No. 5) among the catalysts tested. Fe/Mg₃Al-M prepared from Fe(NH₄)₂(SO₄)₂·6H₂O showed higher activity than Fe-MCM-41-DHT which was previously reported to be highly active for the B–V oxidation, where the optimum Fe loading was around 1.0 wt% (Run No. 14) [28].

3.4. Effect of the preparation method

Either increase or decrease in the calcination temperature of Mg₃Al-HT from 1123 K resulted in a clear decrease in the activity (Run Nos. 5–7). The calcinations of Mg₃Al-HT at both 923 and 1123 K caused the formation of Mg(Al)O periclase, while that at 1223 K enhanced the formation of MgAl₂O₄ spinel additionally to periclase. After dipping the calcined samples in an aqueous solution of Fe(NH₄)₂(SO₄)₂·6H₂O, the reconstitution of hydrotalcite was most intensive for the sample calcined at 1123 K. The Fe loading was highest for the calcination at 923 K, followed by 1123 K and then by 1223 K. Moreover, either increase or decrease in the Mg/Al ratio from 3/1 in Fe/MgAl-M catalyst resulted in a slight decrease in the activity, whereas the Fe loading increased (Run Nos. 5, 8 and 9). This is probably due to the fact that Mg–Al hydrotalcite is stabilized at the Mg/Al ratio around 3/1 as observed in the XRD [48]. Actually after dipping the calcined sample in an aqueous solution of Fe(NH₄)₂(SO₄)₂·6H₂O, the reconstitution of hydrotalcite was most intensively enhanced for the sample of Mg/Al = 3/1, resulting in the highest activity. Thus, it was indicated that the activity was uniquely enhanced by the “memory effect,” irrespective of the Fe loading.

When the Fe loading on Mg₃Al-HT was varied, yield of ϵ -caprolactone increased with increasing Fe loading, reached the maximum value around 6 wt% and further increase in the Fe loading was accompanied by decrease in the yield (Fig. 3). This clearly indicates that an optimum loading existed, where an optimum Fe coordination structure as the active sites is probably attained. Fe/MgO showed higher activity than Fe/ γ -Al₂O₃ (Table 2, Run Nos. 15 and 16); Mg–Fe hydrotalcite structure was formed during the preparation of Fe/MgO, which probably affected the catalytic activity for the B–V oxidation by controlling the coordination sphere around Fe (vide infra), whereas the amount detected by XRD was small. Moreover, the high activity of Fe/MgO may be also assisted by MgO as base [23,24]. The amounts of Fe in two types of iron oxide, Fe₃O₄ and Fe₂O₃, were the same as those in both Fe/ γ -Al₂O₃ and Fe/MgO used in the reactions. Among the two iron oxides, Fe₂O₃ showed higher activity than Fe₃O₄, suggesting that Fe(III) species are more effective than Fe(II) species for the B–V oxidation (Table 2, Run Nos. 17 and 18).

Table 2
Baeyer–Villiger oxidation of cyclohexanone over metal loaded MgAl-HT catalyst^a

Run No.	Catalyst	Metal loading (wt%)	Cyclohexanone conversion (%)	ϵ -Caprolactone yield (%)
1	Fe/Mg ₃ Al-M ^b	9.6	59	58
2	Co/Mg ₃ Al-M ^b	2.4	70	69
3	Ni/Mg ₃ Al-M ^b	4.1	74	72
4	Cu/Mg ₃ Al-M ^b	2.2	90	85
5	Fe/Mg ₃ Al-M ^c	6.1	>99	>99
6	Fe/Mg ₃ Al-M ^{c,d}	10.2	95	68
7	Fe/Mg ₃ Al-M ^{c,e}	4.1	99	74
8	Fe/Mg ₁ Al-M ^c	10.3	99	98
9	Fe/Mg ₆ Al-M ^c	8.0	98	97
10	Fe/Mg ₃ Al-M ^f	11.1	40	36
11	Fe/Mg ₃ Al-M ^g	6.4	48	47
12	Fe/Mg ₃ Al-CP	7.9	96	60
13	Fe/Mg ₂ Al-CP	6.9	85	82
14	Fe-MCM-41-DHT	1.0	80	77
15	Fe/MgO	8.7	98	80
16	Fe/ γ -Al ₂ O ₃	8.5	35	15
17	Fe ₂ O ₃	–	92	90
18	Fe ₃ O ₄	–	84	70
19	Mg ₃ Al-HT	–	25	23
20	Blank	–	10	6

^a Catalyst, 50 mg; acetonitrile, 10 ml; cyclohexanone, 1 mmol; benzaldehyde, 3 mmol; O₂, 10 ml min⁻¹; reaction temperature, 318 K; reaction time 15 h.

^b Mg₃Al(cal.) was dipped for 15 min in aqueous solution of the nitrate of each metal at pH 1.5 for Fe and at pH 3.0 for Co, Ni and Cu.

^c Mg₃Al(cal.) was dipped in aqueous solution of Fe(NH₄)₂(SO₄)₂·6H₂O for 60 min at pH 3.0.

^d Mg₃Al-HT was calcined at 923 K for 5 h.

^e Mg₃Al-HT was calcined at 1223 K for 5 h.

^f Mg₃Al-HT as synthesized was dipped in aqueous solution of 0.03 M for 60 min Fe(NO₃)₂·9H₂O at pH 1.5.

^g Mg₃Al-HT as synthesized was dipped in aqueous solution of 0.03 M for 60 min Fe(NH₄)₂(SO₄)₂·6H₂O at pH 3.0.

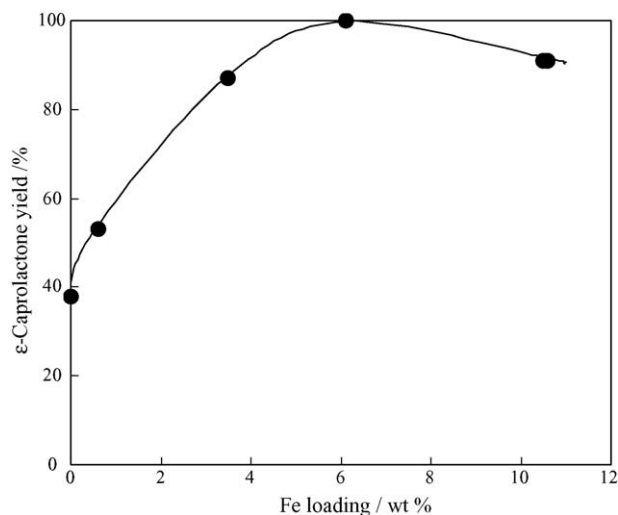


Fig. 3. Effect of Fe loading on the B–V oxidation of cyclohexanone. Fe/Mg₃Al-M, 50 mg; cyclohexanone, 1 mmol; acetonitrile, 10 ml; benzaldehyde, 3 mmol; O₂, 10 ml min⁻¹; reaction temperature, 318 K; reaction time, 15 h.

The effect of preparation method was significant; i.e. coprecipitation afforded the Fe catalyst on which Fe species were well dispersed [32], but the activities were not as high as those of the catalyst prepared by the “memory effect” in the present work (Table 2, Run Nos. 12 and 13). When Mg₃Al-HT as synthesized was used as the catalyst support for dipping, the activities were lower whether Fe(NO₃)₃·9H₂O or Fe(NH₄)₂(SO₄)₂·6H₂O was used (Table 2, Run Nos. 10 and 11) compared with the use of Mg₃Al mixed oxide after calcination. This is probably due to the absence of “memory effect” where Fe species are simply supported on Mg₃Al-HT. These also strongly indicate that the method adopting the “memory effect” is important for the preparation of Fe catalyst for the B–V oxidation.

3.5. Coordination sphere around Fe on Fe/Mg₃Al-M

Diffuse reflectance UV–vis spectra of Fe/Mg₃Al-HT with various Fe content prepared by the “memory effect” using Fe(NH₄)₂(SO₄)₂·6H₂O are shown in Fig. 4. Grünert and co-workers [49] reported that the bands observed above 400 nm are assigned to aggregate large-sized iron oxides particles, while those observed between 300 and 400 nm belong to oligomeric clusters, in the spectra of Fe-ZSM-5. Monomeric iron oxide is observed below 300 nm; the bands at ~220 and ~285 nm are ascribed to Fe³⁺ ← O charge transfer bands of isolated iron ions in tetrahedral and octahedral coordination, respectively (t₁ → t₂/t₁ → e transition unresolved). Centi and Vazzana [50] also observed absorption bands at 270 and 330 nm in the UV–vis spectra of Fe/ZSM-5 samples prepared by CVD and assigned these bands to isolated Fe³⁺ species. In the present work, use of 0.001 M of Fe solution resulted in an appearance of absorption band at 270 nm assigned to isolated Fe³⁺ species interacting strongly with the support (Fig. 4a) [50]. With increasing Fe concentration, new broad bands appeared and were intensified at a wavelength above 300 nm. For the Fe concentration above 0.01 M (3.5 wt% Fe), a shoulder around 500 nm appeared and

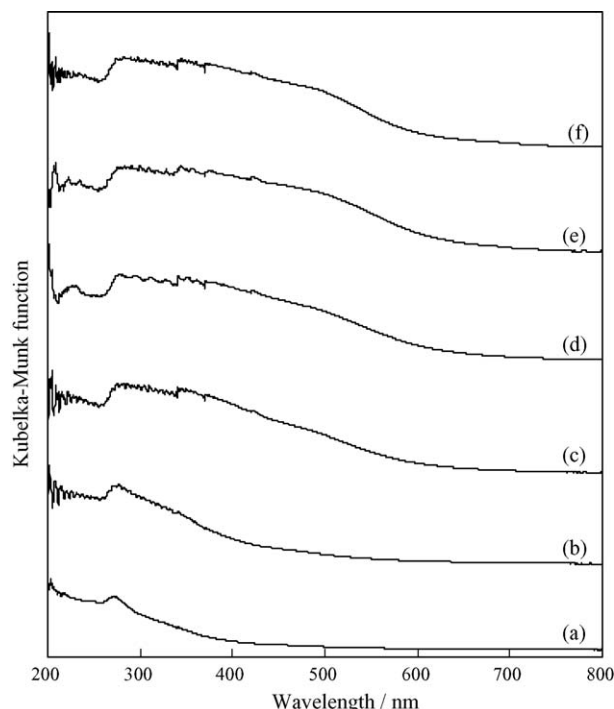


Fig. 4. UV–vis spectra of Fe/Mg₃Al-M catalysts prepared in varying Fe concentrations. (a) 0.001 M, (b) 0.005 M (1.5 wt%), (c) 0.01 M (3.5 wt%), (d) 0.03 M (6.1 wt%), (e) 0.1 M (10.6 wt%) and (f) 0.3 M (10.6 wt%).

was strengthened with increasing Fe concentration (Fig. 4c and e), which is assigned to aggregate large-sized iron clusters [49]. No significant change in the spectra was observed between 0.1 and 0.3 M, since Fe contents in both catalysts were 10.6 wt% (Fig. 4e and f). It is concluded that the most active catalyst, Fe(6.1 wt%)/Mg₃Al-M, showed the most intensive adsorption between 300 and 400 nm assigned to oligomeric Fe clusters.

Fig. 5 shows the Fe K-edge XANES spectra and their first derivatives for Fe(10.3 wt%)/Mg₁Al-M, Fe(6.1 wt%)/Mg₃Al-M and Fe(8.0 wt%)/Mg₆Al-M, along with Fe₂O₃ and Fe(7.9 wt%)/Mg₃Al-CP. The XANES spectra exhibit a pre-edge peak at approximately 7107 eV, which is 10 eV below the inflection point of the adsorption edge (Fig. 5A). The pre-edge peak is assigned to 1s–3d transition, which is dipole-forbidden. Principally, this forbidden transition gains additional intensity when the iron is in a noncentral symmetric environment or through mixing of 3d and 4p orbitals caused by the breakdown of inversion symmetry due to the structure distortion. The peak intensity is closely related to the symmetry around Fe atoms; i.e. this peak becomes more intense as the symmetry is distorted from a regular octahedron [51,52]. Each pre-edge peak area of Fe(10.3 wt%)/Mg₁Al-M, Fe(6.1 wt%)/Mg₃Al-M and Fe(8.0 wt%)/Mg₆Al-M was slightly larger than that of octahedral Fe³⁺ compound, such as α-Fe₂O₃. However, the pre-edge peak area was smaller than that of Fe-MFI whose local structure around Fe is an FeO₄ tetrahedron [53]. These results strongly suggest that Fe atoms in Fe(10.3 wt%)/Mg₁Al-M, Fe(6.1 wt%)/Mg₃Al-M and Fe(8.0 wt%)/Mg₆Al-M are located at a center of a distorted octahedron. If one judges the relative intensities of the pre-edge peak for Fe(10.3 wt%)/Mg₁Al-M,

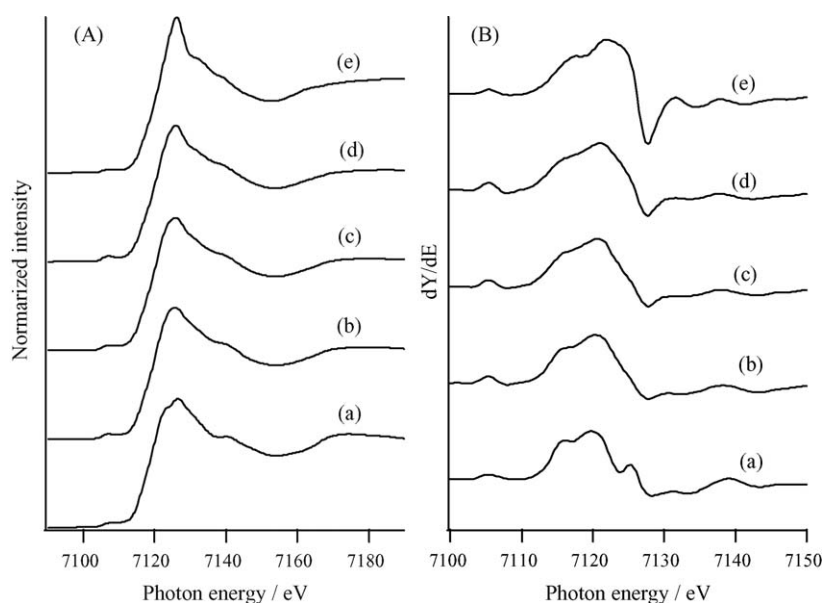


Fig. 5. Fe K-edge XANES spectra (A) and the first differential (B) of supported Fe catalysts and α -Fe₂O₃. (a) α -Fe₂O₃, (b) Fe(10.3 wt%)/Mg₃Al-M, (c) Fe(6.1 wt%)/Mg₃Al-M, (d) Fe(8.0 wt%)/Mg₆Al-M and (e) Fe(7.9 wt%)/Mg₃Al-CP.

Fe(6.1 wt%)/Mg₃Al-M and Fe(8.0 wt%)/Mg₆Al-M against those of Fe₂O₃ and Fe(7.9 wt%)/Mg₃Al-CP, one will see that the distortion of iron in octahedral coordination is larger than in Fe(7.9 wt%)/Mg₃Al-CP. The edge energy shows that Fe in all samples shown in Fig. 5 was in the trivalent state. This can be more clearly seen as a peak around 7115 eV in the first differential Fe K-edge XANES spectra (Fig. 5B).

3.6. Electronic state of Fe on Fe/Mg₃Al-M

The color of the supported Fe catalysts is shown in Table 1 since it is a simple indication of whether bulk iron oxide exists or not [54]. Both as-synthesized Mg₃Al-HT and calcined Mg₃Al samples exhibited a white color (Lot Nos. 1 and 2), while both Fe(7.9 wt%)/Mg₃Al-CP and Fe(6.9 wt%)/Mg₂Al-CP prepared by coprecipitation showed light ochre color, suggesting that iron cations are substantially incorporated inside the framework of hydrotalcite after the coprecipitation (Lot Nos. 15 and 16). The colors of impregnated catalysts, Fe/ γ -Al₂O₃ and Fe/MgO, were also light ochre, indicating that iron species were well dispersed on the supports (Lot Nos. 18 and 19). Fe(9.6 wt%)/Mg₃Al-M and Fe(11.1 wt%)/Mg₃Al-M prepared in the nitrate solution showed brown color, which means that Fe species were sep-

arated from the supports and existed as the oxides (Lot Nos. 3 and 7). Both Ni and Cu/Mg₃Al-M exhibited light green and light blue color, respectively, whereas Co/Mg₃Al-M showed dark grey color. XRD results confirmed that Fe, Co, Ni and Cu/Mg₃Al-M prepared in metal nitrate solutions reconstituted hydrotalcite-like layered structure on Mg₃Al mixed oxide (vide supra). It is known that Co²⁺ [55–58], Ni²⁺ [56] and Cu²⁺ [58] form hydrotalcite-like layered structure with Al³⁺; moreover, the reconstitution takes place for Mg₃Al mixed oxide via dissolution of Mg²⁺ in acidic aqueous solution [35–37]. Therefore, it is most likely that Mg-Al hydrotalcite-like layered structures were reconstituted by substituting the Mg sites with Co²⁺, Ni²⁺ and Cu²⁺ ions. These are also supported by the ionic radii of Co²⁺ (0.745 nm), Ni²⁺ (0.69 nm) and Cu²⁺ (0.73 nm), which are close to that of Mg²⁺ (0.72 nm) all in octahedral coordination [59]. However, it is unlikely that either Fe³⁺ (0.645 nm) or Fe²⁺ (0.78 nm) [59] directly replace the Mg²⁺ sites via “memory effect” on Mg(Al)O periclase due to difference in valence state or ionic radii; a combination of Mg²⁺-Fe³⁺ alone was allowed to form hydrotalcite-like layered structure by coprecipitation starting from the nitrates of Mg²⁺ and Fe³⁺ [41–43]. Actually iron species observed for Fe/Mg₃Al-M possessed the Fe³⁺ valence state even when Mg₃Al mixed oxide was immersed

Table 3
Mössbauer parameters of the supported Fe catalysts

Catalyst	Isomer shift (mm s ⁻¹)	Quadrupole splitting (mm s ⁻¹)	Line-width (mm s ⁻¹)	Spectral contribution (%)	Phases by XRD and UV-vis
Fe(7.9 wt%)/Mg ₃ Al-CP	0.41	0.74	0.37	59	Hydrotalcite
	0.24	0.76	0.37	41	Hydrotalcite
Fe(3.5 wt%)/Mg ₃ Al-M	0.32	0.63	0.62	68	Hydrotalcite
	0.21	0.86	0.62	32	–
Fe(6.1 wt%)/Mg ₃ Al-M	0.34	0.69	0.58	94	Hydrotalcite
	0.46	1.24	0.58	6	Fe ³⁺ clusters

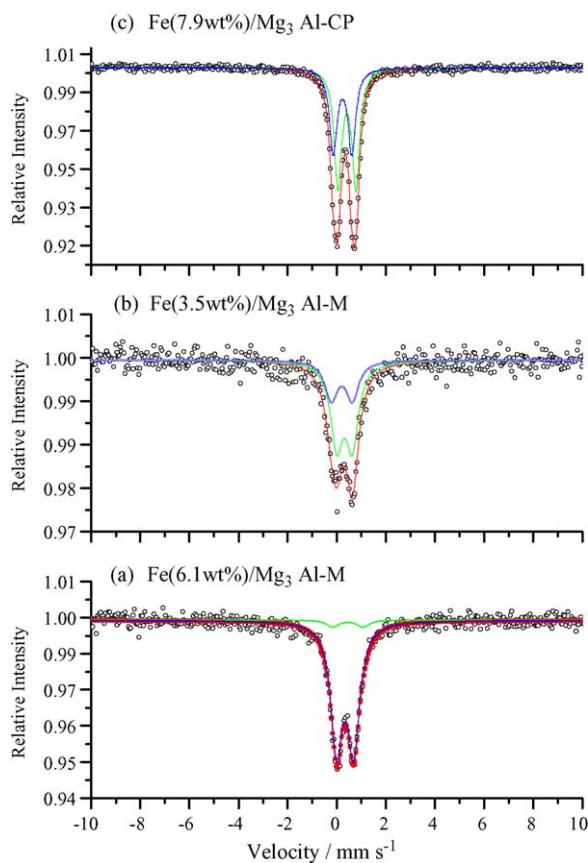


Fig. 6. Mössbauer spectra of supported Fe catalysts. (a) Fe(6.1 wt%)/Mg₃Al-M, (b) Fe(3.5 wt%)/Mg₃Al-M and (c) Fe(7.9 wt%)/Mg₃Al-CP.

in aqueous solution of Fe(NH₄)₂(SO₄)₂·6H₂O containing Fe²⁺ (vide infra).

Mössbauer spectra of Fe(7.9 wt%)/Mg₃Al-CP, Fe(3.5 wt%)/Mg₃Al-M and Fe(6.1 wt%)/Mg₃Al-M and those calculated parameters are shown in Fig. 6 and Table 3, respectively. Both Fe(7.9 wt%)/Mg₃Al-CP and Fe(3.5 wt%)/Mg₃Al-M displayed a doublet with an isomer shift (IS) of 0.21–0.41 mm s⁻¹ and with a quadrupole splitting (QS) of 0.63–0.86 mm s⁻¹; such values are typical of superparamagnetic Fe³⁺ species. The spectrum of Fe(7.9 wt%)/Mg₃Al-CP can be fitted by two doublets; both are attributed to the Fe³⁺ in Mg-Al(Fe) hydrotalcite formed by coprecipitation. Sanchez-Valente et al. [60] reported that the spectra of Mg-Fe hydrotalcite were fitted by two doublets, the parameters of which are IS = 0.33–0.39 mm s⁻¹ and QS = 0.54–0.92 mm s⁻¹ depending on the preparation methods and could be attributed to Fe³⁺ in the hydrotalcite lattice. Shen et al. [42] reported that Mg₃Fe hydrotalcite displays a doublet Fe³⁺ (IS = 0.34 mm s⁻¹) with QS = 0.5 mm s⁻¹. After the calcination at 673 K, the sample exhibited a doublet of Fe³⁺ (IS = 0.28 mm s⁻¹) with QS = 0.67 mm s⁻¹, indicating that the hydrotalcite structure decomposed to form the Mg-Fe mixed oxide [42]. Therefore, the doublets observed as main components in Fe(3.5 wt%)/Mg₃Al-M and Fe(6.1 wt%)/Mg₃Al-M can also be assigned to the Fe³⁺ in the Mg-Fe hydrotalcite formed by the “memory effect” on Mg-Al mixed oxide particles judging from the parameters. The values of IS = 0.21 mm s⁻¹ and

QS = 0.86 mm s⁻¹ observed for Fe(3.5 wt%)/Mg₃Al-M were rather close to those observed for Mg-Fe mixed oxide, i.e. Mg(Fe,Al)O periclase, obtained by the decomposition of Mg-Fe hydrotalcite [42], whereas XRD observation showed no clear evidence probably due to its amorphous character. The color of Fe(3.5 wt%)/Mg₃Al-M was ochre, whereas that of Fe(6.1 wt%)/Mg₃Al-M was dark ochre, indicating that iron species were more condensed on the latter than on the former. Actually, quite different values of IS = 0.46 mm s⁻¹ and QS = 1.24 mm s⁻¹ were observed for Fe(6.1 wt%)/Mg₃Al-M, and can be attributed to Fe³⁺ clusters (vide infra).

3.7. Active sites on Fe/Mg₃Al-M

The doublets observed as the minor component in the Mössbauer spectra of Fe(6.1 wt%)/Mg₃Al-M exhibited higher value of QS = 1.24 mm s⁻¹ compared with those of the other components (Table 3), which is probably attributed to Fe³⁺ cluster-type compounds formed on the surface of Mg-Al mixed oxides. High QS value was also observed for the doublet (1.69 mm s⁻¹) assigned to Fe³⁺ species deposited on finely powdered Ni(II) hydroxide from an aqueous solution of Fe³⁺ nitrate in the presence of NaOH [61,62]. This high QS value is uniquely due to the high ratio of Fe to Ni where ferric ions link by oxy- and hydroxyl-bridging bonds to form the cluster-type compounds [63]. In the study on synthetic and natural pyroaurite, i.e. Mg²⁺-Fe³⁺ hydrotalcite, it is reported that QS in general can be considered as derived from two idealized contributions: one characteristic for Fe with only Mg as nearest neighbours dominant in the Fe-poor samples, and another where Fe has one or several neighbours of Fe (cluster-type arrangements). The former is characterized by QS of approximately 0.5 mm s⁻¹ and explains the almost constant QS found for low Fe contents, whereas the latter and minor component has QS of approximately 0.9 mm s⁻¹ [64]. The high QS value obtained for Fe(6.1 wt%)/Mg₃Al-M is also likely due to the formations of cluster-type Fe³⁺ species. This is supported by the results of UV-vis observations (Fig. 4) as well as the dark ochre color of Fe(6.1 wt%)/Mg₃Al-M (Table 1), indicating the formations of aggregated Fe³⁺ species. It is most likely that Fe³⁺ clusters significantly improved the activity of Fe/MgAl-M catalysts.

The *k*³-weighted EXAFS functions (A) and the corresponding Fourier transforms (B) for supported Fe catalysts are shown in Fig. 7. EXAFS spectra of Fe/MgAl-CP and Fe/MgAl-M are obviously different from those of α-Fe₂O₃, indicating that the local structure of most Fe³⁺ species is different from that in α-Fe₂O₃. Among the supported Fe catalysts, all three Fe/MgAl-M catalysts showed similar EXAFS spectra, whereas EXAFS spectra for Fe/MgAl-CP are distinguished from those of Fe/MgAl-M, suggesting that the local structures are different with each other for Fe/MgAl-CP and Fe/MgAl-M catalysts. Fourier transforms (B) showed two peaks at 1.5 and 2.7 Å (phase shift uncorrected); the former is attributed to Fe–O bonding and the latter to Fe–O–Fe bonding. The results of curve-fitting analysis are summarized in Table 4. The first coordination spheres for all the samples could be fit with two shells. Although their Fe–O dis-

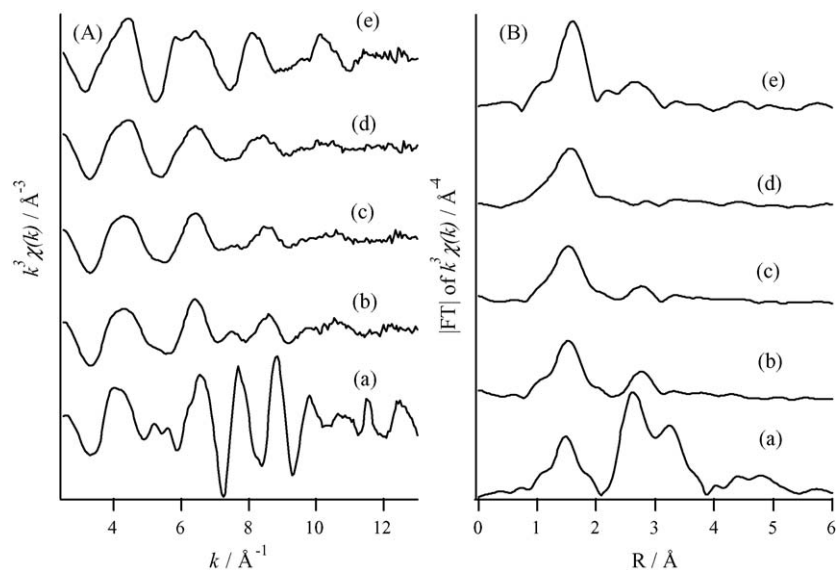


Fig. 7. The k^3 -weighted EXAFS functions (A) and the k^3 -weighted Fourier transforms (B) for supported Fe catalysts and α -Fe₂O₃. (a) α -Fe₂O₃, (b) Fe(10.3 wt%)/Mg₁Al-M, (c) Fe(6.1 wt%)/Mg₃Al-M, (d) Fe(8.0 wt%)/Mg₆Al-M and (e) Fe(7.9 wt%)/Mg₃Al-CP.

tances were slightly shorter than those in α -Fe₂O₃, coordination numbers are similar to those of α -Fe₂O₃, whose coordination environment is six-fold. This indicates that Fe atoms in all the catalysts are present at the center of oxygen octahedron. For both Fe(10.3 wt%)/Mg₁Al-M and Fe(6.1 wt%)/Mg₃Al-M catalysts, the average coordination number for Fe–O–Fe was around 2.0, suggesting that three nuclear or second dimensionally grew clusters were formed on the Fe/MgAl-M catalysts. The curve-fitting was not easy for Fe(8.0 wt%)/Mg₆Al-M due to too weak signal around 2.7 Å. For the Fe(7.9 wt%)/Mg₃Al-CP catalyst, the peaks around 2.7 Å could not be fit with Fe–Fe shell, suggesting that the scattering atom at the second coordination sphere

is not only Fe but also Mg or Al derived from the hydrotalcite structure.

3.8. Catalytic behavior of Fe(6.1 wt%)/Mg₃Al-HT

The catalytic behavior of Fe(6.1 wt%)/Mg₃Al-M in the B–V oxidation of cyclohexanone with various oxidizing agents are shown in Table 5. The highest yield of ϵ -caprolactone was obtained with the oxygen and benzaldehyde coupled system (Run No. 1). Use of molecular oxygen (Run No. 2), hydrogen peroxide (Run No. 3) or *t*-butyl hydroperoxide (Run No. 4) was not effective even in the presence of Fe(6.1 wt%)/Mg₃Al-M catalyst, and *m*-CPBA afforded high yield of ϵ -caprolactone (Run No. 5). However, *m*-CPBA alone could not work as oxidizing agent in the absence of catalyst (Run No. 6). These clearly suggest that the active oxygen species must be peracid, which is activated on the Fe³⁺ clusters as the active Lewis acid site and oxidizes cyclohexanone to ϵ -caprolactone.

Table 4
Parameters obtained from EXAFS analysis for the supported Fe catalysts

Catalysts	Shell	C.N. ^a	R (Å) ^b	σ (Å) ^c	R
Fe(7.9 wt%)/Mg ₃ Al-CP	O	3.1	1.87	0.082	7.7
		3.1	1.99	0.086	
Fe(10.3 wt%)/Mg ₁ Al-M	O	2.7	1.87	0.088	6.9
		2.8	2.00	0.092	
Fe(6.1 wt%)/Mg ₃ Al-M	Fe	2.5	3.06	0.102	1.5
		2.8	2.01	0.112	
Fe(6.1 wt%)/Mg ₃ Al-M	O	2.8	1.86	0.102	6.9
		2.8	2.01	0.112	
Fe(8.0 wt%)/Mg ₆ Al-M	O	1.8	3.07	0.114	2.6
		3.0	1.87	0.098	
Fe(8.0 wt%)/Mg ₆ Al-M	O	3.1	2.06	0.096	3.7
		3.0	1.95	0.098	
α -Fe ₂ O ₃ ^d	O	3.0	1.95	0.098	3.7
		3.0	2.12	0.112	
α -Fe ₂ O ₃ ^d	Fe	1.0	2.90	0.114	2.6
		3.0	2.97	0.112	

^a C.N.: coordination number.

^b R : interatomic distance.

^c σ^2 : Debye–Waller factors.

^d Data from X-ray crystallography.

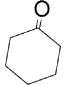
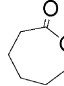
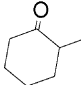
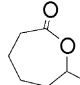
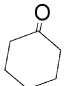
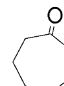
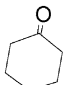

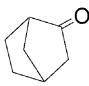
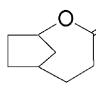
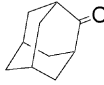
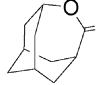
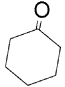
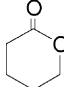
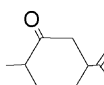
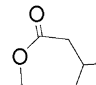
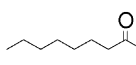
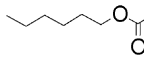
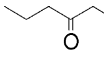
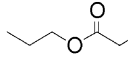
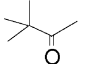
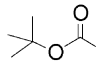
Table 5
Baeyer–Villiger oxidation of cyclohexanone with various oxidizing agent over Fe/Mg₃Al-M catalyst^a

Run No.	Oxidizing agent	Cyclohexanone conversion (%)	ϵ -Caprolactone yield (%)
1	O ₂ /benzaldehyde	>99	>99
2	O ₂	0	0
3	H ₂ O ₂	0	0
4	<i>t</i> -BuOOH	0	0
5	<i>m</i> -CPBA	97	92
6	<i>m</i> -CPBA ^b	0	0

^a Fe(6.1 wt%)/Mg₃Al-M catalyst, 50 mg; dimethylformamide, 10 ml; cyclohexanone, 1 mmol; H₂O₂, 5 mmol; *t*-BuOOH, 3 mmol; *m*-CPBA, 3 mmol; benzaldehyde, 3 mmol; O₂, 10 ml min⁻¹; reaction temperature, 318 K; reaction time, 15 h.

^b In the absence of catalyst.

Table 6
Baeyer–Villiger oxidation of various ketones^a

Run No.	Ketone	Product	Yield (%)
1			>99
2			>99
3			93
4			46
5			>99
6			>99
7			43
8			Trace
9			Trace
10			Trace
11			Trace

^a Fe(6.1 wt%)/Mg₃Al-M catalyst, 50 mg; dimethylformamide, 10 ml; ketone, 1 mmol; benzaldehyde, 3 mmol; O₂, 10 ml min⁻¹; reaction temperature, 318 K; reaction time, 15 h.

When various ketones were used as the substrates for the B–V oxidation with the Fe(6.1 wt%)/Mg₃Al-HT catalyst (Table 6), cyclic ketones were more efficiently oxidized than linear ketones. Among the cyclic ketones, six-membered cyclic and bicyclic ketones were most efficiently oxidized to the corresponding lactones. However, alkyl substitution to the ring of cyclic ketones retarded the oxidation; increasing bulkiness of the substituents caused significant retardation of the oxidation.

Effect of the catalyst removal during the reaction is shown in Fig. 8. The B–V oxidation proceeded smoothly in the presence of Fe(6.1 wt%)/Mg₃Al-M catalyst; cyclohexanone was almost perfectly converted to ε-caprolactone within 15 h. At the reaction time of 3 h after starting the reaction, the catalyst was removed

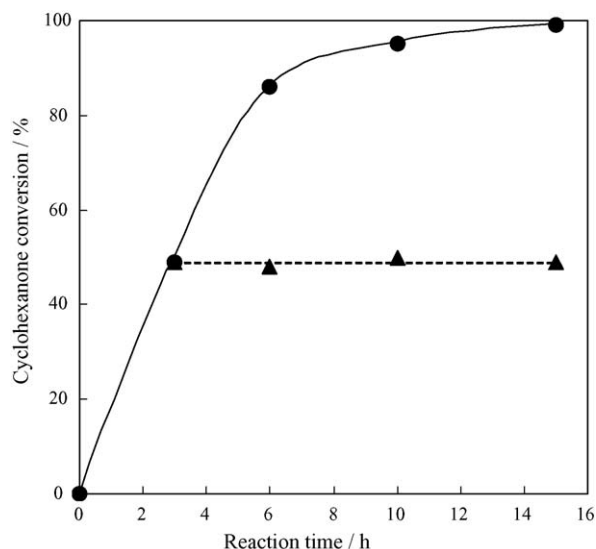


Fig. 8. Effect of catalyst removal during the B–V oxidation. Fe(6.1 wt%)/Mg₃Al-M, 50 mg; cyclohexanone, 1 mmol; acetonitrile, 10 ml; benzaldehyde, 3 mmol; O₂, 10 ml min⁻¹; reaction temperature, 318 K. (—) In the presence of catalyst and (---) after removal of catalyst.

by filtration of the reaction solution and the reaction was followed with the filtrate. After the catalyst removal, the reaction did not proceed at all, indicating that the B–V oxidation was heterogeneously catalyzed on the improved Fe/Mg₃Al-M catalyst.

4. Conclusion

Fe containing Mg–Al hydrotalcite-type anionic clay phase has been prepared on the surface of Mg₃Al mixed oxide by adopting the “memory effect” of hydrotalcite. Mg–Al hydrotalcite was calcined to the mixed oxide and dipped in an aqueous solution of Fe(NH₄)₂(SO₄)₂·6H₂O, the pH of which was adjusted to 3.0; Fe species was incorporated by the “memory effect” to form Fe/Mg₃Al hydrotalcite as the active phase on the surface of the Mg₃Al mixed oxide. The Fe/Mg₃Al-M catalyst showed high activity for the Baeyer–Villiger oxidation of ketones with benzaldehyde and O₂. The Fe/Mg₃Al-M catalyst showed higher activity than those prepared by coprecipitation from the nitrates of Mg, Fe and Al. Judging from the Mössbauer and Fe K-edge XAFS spectra, Fe species possess the Fe³⁺ valence state, are mainly octahedrally coordinated and formed cluster-type structure on the Mg–Al mixed oxides. It is most likely that the cluster structure containing Fe³⁺–O–Fe³⁺ species was formed on the catalyst surface, which worked as the active sites for the Baeyer–Villiger oxidation. This species was more active than well dispersed Fe³⁺ species formed on the hydrotalcite prepared by coprecipitation. Six-membered cyclic ketones, such as cyclohexanone, 2-norbornone and 2-adamantanone, were effectively oxidized to the corresponding lactones.

References

- [1] G.R. Krow, Org. React. 43 (1993) 251.
- [2] G. Strukul, Angew. Chem. Int. Ed. 37 (1998) 1198.
- [3] M. Renz, B. Meunier, Eur. J. Org. Chem. (1999) 737.

- [4] A. Corma, L.T. Nemeth, M. Renz, S. Valencia, *Nature* 412 (2001) 423.
- [5] U.R. Pillai, E. Sahle-Demessie, *J. Mol. Catal. A* 191 (2003) 93.
- [6] C.-M. Che, J.-S. Huang, *Coord. Chem. Rev.* 242 (2003) 97.
- [7] G. Strukul, A. Varagnolo, F. Pinna, *J. Mol. Catal. A* 117 (1997) 413.
- [8] T. Uchida, T. Katsuki, *Tetrahedron Lett.* 42 (2001) 6911.
- [9] K. Mikami, M.N. Isslam, M. Yamanaka, Y. Itoh, M. Shinoda, K. Kudo, *Tetrahedron Lett.* 45 (2004) 3681.
- [10] B.M. Trost, *Science* 254 (1991) 1471.
- [11] P.T. Anastas, J.C. Warner, *Green Chemistry: Theory and Practice*, Oxford University Press, 1998.
- [12] J.H. Clark, *Green Chem.* 1 (1999) 1.
- [13] J. Fisher, W.F. Hölderich, *Appl. Catal. A* 180 (1999) 435.
- [14] C. Palazzi, F. Pinna, G. Strukul, *J. Mol. Catal. A* 151 (2000) 245.
- [15] B.M. Choudary, Ch. Sridhar, M. Sateesh, B. Sreedhar, *J. Mol. Catal. A* 212 (2004) 237.
- [16] A. Corma, L.T. Nemeth, M. Renz, S. Valencia, *Nature* 412 (2001) 423.
- [17] A. Corma, V. Fornés, S. Iborra, M. Mifsud, M. Renz, *J. Catal.* 221 (2004) 67.
- [18] A. Corma, S. Iborra, M. Mifsud, M. Renz, *J. Catal.* 234 (2005) 96.
- [19] Z. Lei, Q. Zhang, J. Luo, X. He, *Tetrahedron Lett.* 46 (2005) 3505.
- [20] U.R. Pillai, E. Sahle-Demessie, *J. Mol. Catal.* 191 (2003) 93.
- [21] S.-I. Murahashi, Y. Oda, T. Naota, *Tetrahedron Lett.* 33 (1992) 7557.
- [22] K. Kaneda, S. Ueno, T. Imanaka, E. Shimotsuma, Y. Nishiyama, Y. Ishii, *J. Org. Chem.* 59 (1994) 2915.
- [23] K. Kaneda, S. Ueno, T. Imanaka, *J. Chem. Soc., Chem. Commun.* (1994) 797.
- [24] K. Kaneda, S. Ueno, T. Imanaka, *J. Mol. Catal. A* 102 (1995) 135.
- [25] I.C. Chisem, J. Chisem, J.H. Clark, *New J. Chem.* (1998) 81.
- [26] R. Raja, J.M. Thomas, G. Sankar, *Chem. Commun.* (1999) 525.
- [27] K. Kaneda, S. Haruna, T. Imanaka, K. Kawamoto, *J. Chem. Soc., Chem. Commun.* (1990) 1467.
- [28] T. Kawabata, Y. Ohishi, S. Itsuki, N. Fujisaki, T. Shishido, K. Takaki, Q. Zhang, Y. Wang, K. Takehira, *J. Mol. Catal. A* 236 (2005) 99.
- [29] T. Kawabata, Y. Shinozuka, Y. Ohishi, T. Shishido, K. Takaki, K. Takehira, *J. Mol. Catal. A* 236 (2005) 206.
- [30] N.I. Sax, *Dangerous Properties of Industrial Materials*, sixth ed., Van Nostrand Reinhold Company Inc., New York, 1984.
- [31] F. Cavani, F. Trifiro, A. Vaccari, *Catal. Today* 11 (1991) 173.
- [32] K. Kaneda, S. Ueno, T. Imanaka, *J. Mol. Catal. A* 102 (1995) 135.
- [33] S. Ueno, K. Ebitani, A. Ookubo, K. Kaneda, *Appl. Surf. Sci.* 121/122 (1997) 366.
- [34] F. Kooli, C. Depege, A. Ennanqadi, A. De Roy, J.-P. Besse, *Clays Clay Miner.* 45 (1997) 92.
- [35] J. Rocha, M. Del Arco, V. Rives, M.A. Ulibarri, *J. Mater. Chem.* 9 (1999) 2499.
- [36] M. Rajamathi, G.D. Nataraja, S. Ananthamurthy, P.V. Kamath, *J. Chem. Mater.* 10 (2000) 2754.
- [37] J.A. van Bokhoven, J.C.A.A. Roelofs, K.P. Jong, D.C. Koningsberger, *Chem. Eur. J.* 7 (2001) 1258.
- [38] K. Takehira, T. Shishido, D. Shoro, K. Murakami, M. Honda, T. Kawabata, K. Takaki, *Catal. Commun.* 5 (2004) 209.
- [39] K. Takehira, T. Kawabata, T. Shishido, K. Murakami, T. Oh, D. Shoro, M. Honda, K. Takaki, *Appl. Catal. A* 279 (2005) 41.
- [40] K. Takehira, T. Kawabata, T. Shishido, K. Murakami, T. Oh, D. Shoro, M. Honda, K. Takaki, *J. Catal.* 231 (2005) 92.
- [41] R.S. Mulukutla, C. Detellier, *J. Mater. Sci. Lett.* 15 (1996) 797.
- [42] J. Shen, B. Guang, M. Tu, Y. Chen, *Catal. Today* 30 (1996) 77.
- [43] J.M. Fernández, M.A. Ulibarri, F.M. Labajos, V. Rives, *J. Mater. Chem.* 8 (1998) 2507.
- [44] T. Hibino, A. Tsunashima, *J. Mater. Sci. Lett.* 19 (2000) 1403.
- [45] O.P. Ferreira, O.L. Alves, D.X. Gouveia, A.G.S. Filho, J.A.C. de Paiva, J.M. Filho, *J. Solid State Chem.* 177 (2004) 3058.
- [46] M. Miyata, A. Okada, *Clays Clay Miner.* 25 (1977) 14.
- [47] J.B. Van Zon, D.C. Koningsberger, H.F.J. Van Blik, D.E. Sayers, *J. Phys. Chem.* 82 (1985) 5742.
- [48] F. Cavani, F. Trifiro, A. Vaccari, *Catal. Today* 11 (1991) 173.
- [49] M. Schwidder, M.S. Kumar, K. Klementiev, M.M. Pohl, A. Brückner, W. Grünert, *J. Catal.* 231 (2005) 314.
- [50] G. Centi, F. Vazzana, *Catal. Today* 53 (1999) 683.
- [51] A.C. Roe, D.J. Schneider, R.J. Mayer, J.W. Pyrz, J. Widom Jr., L. Que, *J. Am. Chem. Soc.* 106 (1984) 1676.
- [52] T.E. Westre, P. Kennepohl, J.G. DeWitt, B. Hedman, K.O. Hodgson, E.I. Solomon, *J. Am. Chem. Soc.* 119 (1997) 6297.
- [53] S. Bordiga, R. Buzzoni, F. Geobaldo, C. Lamberti, E. Giamello, A. Zecchina, G. Leofanti, G. Petrini, G. Vlaic, *J. Catal.* 158 (1996) 486.
- [54] P. Ratnasami, R. Kumar, *Catal. Today* 53 (1991) 329.
- [55] E. Scavetta, M. Berrettoni, F. Nobili, D. Tonelli, *Electrochim. Acta* 50 (2005) 3305.
- [56] J. Pérez-Ramírez, G. Mul, J.A. Moulijn, *Vib. Spectrosc.* 27 (2001) 75.
- [57] J. Pérez-Ramírez, G. Mul, F. Kapteijin, J.A. Moulijn, *Mater. Res. Bull.* 36 (2001) 1767.
- [58] L. Chmielarz, R. Kuśtrowski, A. Rafalska-Lasocha, R. Dziembaj, *Thermochim. Acta* 395 (2003) 225.
- [59] R.D. Shannon, *Acta Crystallogr. A* 32 (1976) 751.
- [60] J. Sanchez-Valente, J.M.M. Millet, F. Figueras, L. Fournes, *Hyperfine Inter.* 131 (2000) 43.
- [61] A.A. Kamnev, B.B. Ezhov, V. Rusanov, V. Angelov, *Electrochim. Acta* 37 (1992) 469.
- [62] A.A. Kamnev, Yu.D. Perfilov, *J. Radioanal. Nucl. Chem.* 190 (1995) 321.
- [63] W.E. O'Grady, *J. Electrochem. Soc.* 127 (1980) 555.
- [64] C.B. Koch, *Hyperfine Inter.* 117 (1998) 131.